Brain Struct Funct (2017) 222:1861–1875
DOI 10.1007/s00429-016-1312-z

ORIGINAL ARTICLE

Structural and functional alterations in the prefrontal cortex after post-weaning social isolation: relationship with species-typical and deviant aggression

Laszlo Biro[1,3] · Mate Toth[1] · Eszter Sipos[1] · Biborka Bruzsik[1] · Aron Tulogdi[1] · Samuel Bendahan[2] · Carmen Sandi[2] · Jozsef Haller[1]

Received: 5 May 2016 / Accepted: 13 September 2016 / Published online: 23 September 2016

Abstract Although the inhibitory control of aggression by the prefrontal cortex (PFC) is the cornerstone of current theories of aggression control, a number of human and laboratory studies showed that the execution of aggression increases PFC activity; moreover, enhanced activation was observed in aggression-related psychopathologies and laboratory models of abnormal aggression. Here, we investigated these apparently contradictory findings in the post-weaning social isolation paradigm (PWSI), an established laboratory model of abnormal aggression. When studied in the resident-intruder test as adults, rats submitted to PWSI showed increased attack counts, increased share of bites directed towards vulnerable body parts of opponents (head, throat, and belly) and reduced social signaling of attacks. These deviations from species-typical behavioral characteristics were associated with a specific reduction in the thickness of the right medial PFC (mPFC), a bilateral decrease in dendritic and glial density, and reduced vascularization on the right-hand side of the mPFC. Thus, the early stressor interfered with mPFC development. Despite these structural deficits, aggressive encounters enhanced the activation of the mPFC in PWSI rats as compared to controls. A voxel-like functional analysis revealed that overactivation was restricted to a circumscribed sub-region, which contributed to the activation of hypothalamic centers involved in the initiation of biting attacks as shown by structural equation modeling. These findings demonstrate that structural alterations and functional hyperactivity can coexist in the mPFC of rats exposed to early stressors, and suggest that the role of the mPFC in aggression control is more complex than suggested by the inhibitory control theory.

Keywords Abnormal aggression · Prefrontal cortex · Post-weaning social isolation · c-Fos · Rat

✉ Jozsef Haller
haller.jozsef@koki.mta.hu

[1] Department of Behavioral Neuroscience, Institute of Experimental Medicine, P.O. Box 67, 1450 Budapest, Hungary

[2] Brain Mind Institute, School of Life Sciences, École Polytechnique Federale de Lausanne (EPFL), Lausanne, Switzerland

[3] János Szentágothai School of Neurosciences, Semmelweis University, Budapest, Hungary

Introduction

The inhibitory modulation of aggression by the prefrontal cortex (PFC) is the cornerstone of current theories of aggression control that suggest that dysfunctions in this brain area lead to the development of aggression-related psychopathologies (Glenn et al. 2013; Blair 2015). The most dramatic change observed in brain imaging studies is the reduction of prefrontal gray matter volume in these disorders (Raine et al. 2000; Tiihonen et al. 2008; Ermer et al. 2013). Although widely recognized, several lines of evidence obtained in rodents and humans are at variance with this hypothesis.

Over the last decade, several models of aggression-related psychopathologies were developed in rodents to study the neural underpinnings of escalated (psychopathology-like) aggression (Miczek et al. 2013; Haller et al. 2014). Prefrontal volume was not investigated in these models so far, but findings with neuronal activity markers revealed that aggression increases PFC activation; moreover, enhanced increases in PFC activation were observed in

animals submitted to models of escalated aggression (Halasz et al. 2006; Haller et al. 2006; Beiderbeck et al. 2012; Toth et al. 2012; Ago et al. 2013). In only two of such studies were PFC activations blunted by escalated aggression in some sub-areas of the PFC (Wall et al. 2012; Marquez et al. 2013). However, fighting *per se* did activate the PFC in these studies as well, and activation was reduced but not eliminated by escalated aggression. Likewise, human studies in which the impact of actually performed aggression was studied (e.g., subjects played aggressive video games or retaliated aggressively in competitive situations), the PFC was also found to be activated by aggressive actions (Lotze et al. 2007; Montag et al. 2012); moreover, the activation was stronger in subjects with aggression-related psychopathologies (New et al. 2009; Veit et al. 2010).

Taken together, these findings suggest a duality regarding the involvement of the PFC in aggression control: whereas chronic structural deficits in the PFC increase aggressiveness, aggressive behaviors induce the activation of the very same area. In a first attempt to investigate the putative dual role of PFC in aggression, we submitted rats to post-weaning social isolation (PWSI), an established model of human early social neglect, which is a significant contributor to adult violence and criminality (Gilbert et al. 2009; Haller et al. 2014; Sandi and Haller 2015). PWSI replicates in rats many detrimental effects of human early social neglect including escalated aggression as shown by enhanced bite counts and enhanced shares of bites directed towards vulnerable body parts of opponents (head, throat, belly) (Tóth et al. 2008; Toth et al. 2011; Haller et al. 2014). We studied putative structural deficits induced by PWSI in the medial PFC (mPFC), to investigate whether changes observed in abnormally aggressive humans are reproduced by the model. We also investigated neuronal activation patterns induced by fighting in the same subjects. To capture the spatial correlates of the putative duality of mPFC involvement in aggression control, we developed a high-resolution voxel-like approach. Behaviorally relevant interactions between the mPFC and other brain areas involved in aggressive behavior were investigated by structural equation modeling (SEM).

Materials and methods

Animals

Subjects were male Wistar rats born in the breeding facility of our Institute. Parents originated from a Charles River Laboratories breeding line. Subjects were studied in the resident-intruder test 74 days after birth, when their weight was 400–450 g. Intruders used in aggressive encounters came from the same source and weighed approximately 300 g at testing. These rats were group-housed; each intruder was used only once. For all rats, food and water were available ad libitum throughout, while temperature and relative humidity were kept at 22 ± 2 °C and 60 ± 10 %, respectively. Rats were maintained in a light cycle of 12:12 h with lights off at 0800 h. No rat was handled except for regular cage cleaning. The experiments were carried out in accordance with the European Communities Council Directive of 2010 (2010/63/EU) and were reviewed and approved by the Animal Welfare Committee of the Institute of Experimental Medicine.

Experimental design

Pups were weaned on the 21st postnatal day. During the following 7 weeks, littermates were randomly assigned either to individual housing (post-weaning social isolation, PWSI), or to social housing in groups of 4 (socially reared, SR) in Makrolon cages ($42 \times 26 \times 19$ cm). Each social group contained pups coming from at least three different litters. SR rats were moved to larger Makrolon cages when their weight reached approximately 200 g ($60 \times 38 \times 19$ cm). On the 8th post-weaning week, all subjects were moved to individual cages for 3 days to induce the territorial behavior that is studied in the resident–intruder test. In the early hours of the active (dark) period of the third day, subjects were either submitted to the resident/intruder test, or were left undisturbed in their home cages. Four groups of animals were studied: (1) SR not exposed to the resident–intruder test ($N = 10$), (2) SR studied in the resident–intruder test ($N = 14$), (3) PWSI not exposed to the resident–intruder test ($N = 10$), and (4) PWSI studied in the resident–intruder test ($N = 14$). Three brains were damaged during processing; two belonged to fighting SR whereas one to the fighting PWSI group. These animals were discarded from the study. Ninety minutes after the end of the encounter, all rats were anesthetized, their brains were perfused, and sampled for histological and immunohistochemical procedures.

A second experiment was run to study the neurochemical nature of activated mPFC neurons. The reason of performing this additional experiment was that the mPFC study was performed on sections made between Bregma 3.20 and 2.70 to ensure the comparability of findings obtained with different technologies, and there were no sufficient sections to perform this neurochemistry-oriented investigation. The second experiment was performed under the same, highly standardized conditions. Importantly, the behavioral consequences of PWSI as well as its effect on prefrontal activation were entirely similar to that observed in the first experiment (see below).

Resident–intruder test

Subjects were faced with a smaller intruder (body weight difference was of 30 %) for 20 min in their home cage (a Plexiglas cage measuring 60 × 40 × 50 cm). The test was carried out in the early phase of the dark period under dim red illumination. Behavior was video recorded through the transparent front wall of the cage. Video recordings were evaluated for biting attack episodes by an experimenter blind to treatment conditions, who recorded the number of attacks, their targets on the body of opponents and their behavioral context, i.e., behaviors typically altered by PWSI (Tóth et al. 2008; Toth et al. 2011). Analysis was made at low speed, frame-by-frame when necessary. Attacks were considered vulnerable if targeted the head (areas anterior to the ears), throat (the ventral area below the ears), belly (ventral areas between legs) or paws, and non-vulnerable if targeted the back or flanks (posterior to the ears and dorsal to the legs) of opponents. As regards the behavioral context, an attack was considered signaled if it was preceded by offensive threats (aggressive grooming, mounting, lateral threat, chasing, wrestling, offensive upright) or dominant posture (keeping down the opponent while it is lying on its back), and non-signaled if it was preceded by non-aggressive behaviors (e.g., exploration, grooming, resting, etc.).

Brain processing

Rats were deeply anesthetized with a mixture of ketamine–xylazine–pipolphen (50–10–5 mg/kg) and were perfused through the ascending aorta with 100 ml ice-cold 0.1 M phosphate-buffered saline followed by approximately 200 ml 4 % paraformaldehyde (in 0.1 M phosphate-buffered saline). Brains were removed, post-fixed in the same solution for 3 h and cryoprotected overnight by 20 % sucrose in phosphate-buffered saline at 4 °C. 30-µm frozen sections were cut in the frontal plane on a sliding microtome.

Assessment of structural changes in the mPFC

Structural changes were investigated on two sections 180 µm apart situated between levels 3.20 and 2.70 mm from Bregma (Paxinos and Watson 1998). In this region, the forceps minor is a clearly recognizable closed structure, which allowed the precise measurement of cortical thickness by a method adapted from earlier studies (Day-Wilson et al. 2006; Schubert et al. 2009; Spivey et al. 2009). Rest of the measurements was made at the same mPFC rostrocaudal level for consistency.

The thickness of the medial prefrontal cortex was measured bilaterally on dark-field images. We drew two lines perpendicular to the medial longitudinal fissure; one through the upper, whereas the other through the lower end of the forceps minor of the corpus callosum (for a graphical illustration of the measurement see Fig. 1). The thickness of the medial prefrontal cortex was characterized by the length of these lines. To evaluate changes in forceps minor size, the distance between the lines was also measured. To investigate whether the observed changes were due to an overall change in brain volume, we also estimated the size of the periaqueductal gray (PAG) by delineating the whole central gray area on dark-field images on three consecutive sections 180 µm apart. 'Volumetric' change was estimated by calculating the average PAG areas (mm^2) excluding the aqueductus.

We further assessed neuron and glia counts, dendritic density and the vascularization in the area by staining for the neuronal nuclear antigen (NeuN), glial fibrillary acidic protein (GFAP), neurofilament H (SMI-32), and lectin (as a marker for glycoproteins on the endothelial surface) as described earlier (van Praag et al. 2007; Van De Werd and Uylings 2008; Aksic et al. 2013; Sanada et al. 2014). Free-floating sections were incubated in 0.5 % H_2O_2 with 0.3 % Triton X-100 in phosphate buffer saline (PBS), then blocked by 5 % normal horse or goat serum in PBS (NHS/NGS; Jackson ImmunoResearch) using 10-min PBS rinses between all incubations. In case of SMI-32, permeability was increased by means of liquid nitrogen application without Triton X-100 treatment. Sections were incubated in primary antibody solutions that contained 2.5 % NHS or NGS in PBS (NeuN: 1:5000, MAB377, Millipore; GFAP: 1:2000, G3893, Sigma-Aldrich; SMI-32: 1:1000, NE1023, Millipore) for 48–72 h at 4 °C. Primary antibodies were detected by biotinylated secondary antibodies (1:1000 in PBS with 2.5 % NHS or NGS; Jackson ImmunoResearch) and avidin–biotin complex (ABC, 1:1000; Vector Laboratories) for 1 h each at room temperature in case of NeuN, and SMI-32. The peroxidase reaction was developed in the presence of diaminobenzidine tetrahydrochloride (0.2 mg/ml), nickel–ammonium sulfate (0.1 %) and hydrogen peroxide (0.003 %) dissolved in Tris buffer. Anti-GFAP antibodies were detected by Alexa Fluor 594-conjugated secondary antibody (Life Technologies). Lectin was visualized by a slightly different protocol. Briefly, sections were rinsed in Tris-buffered saline (TBS), permeabilized by 0.3 % Triton X-100, and blocked by 5 % pre-immune donkey serum in TBS for 30 min at room temperature. Lectin was detected by means of 72 h incubation in biotinylated *Lycopersicon esculentum* solution at 4 °C (1:4000 in TBS, L0651, Sigma-Aldrich), which was visualized by streptavidin-Alexa Fluor 488-conjugate (1:1000, Life Technologies). Microscopic images were digitized by an Olympus CCD camera using a 10× magnification lens. Relative optical density was assessed in the same area

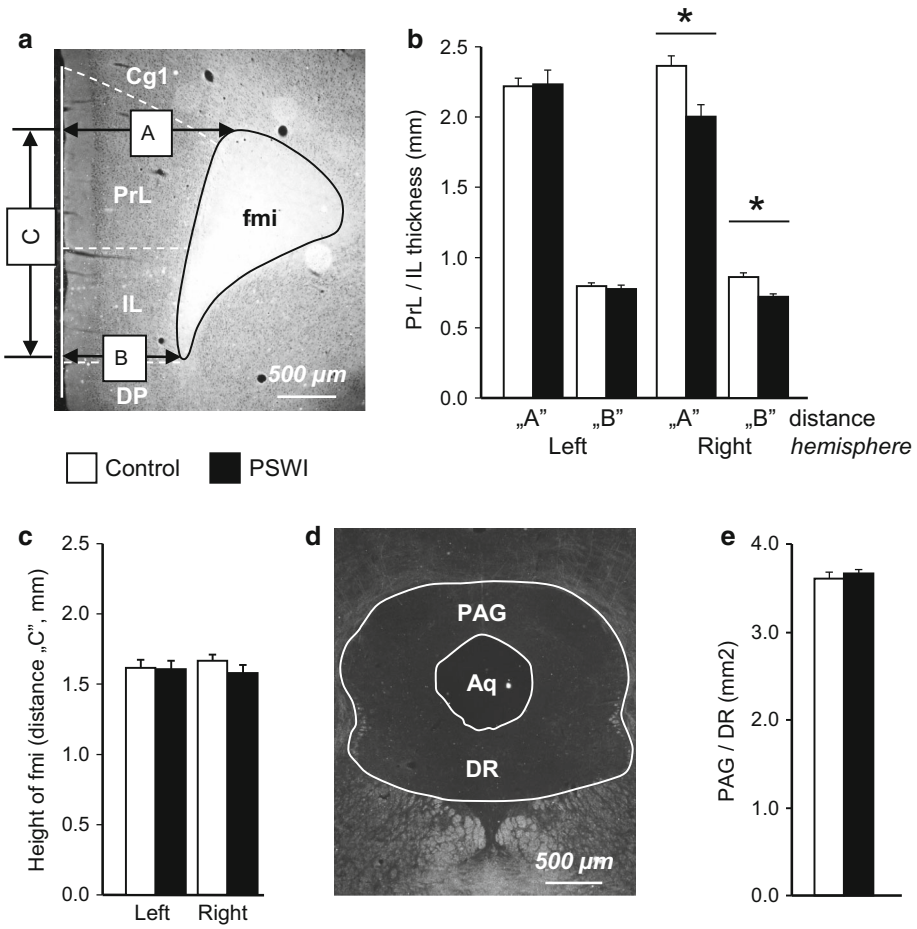

Fig. 1 Changes in the thickness of the mPFC at Bregma 3.20–2.70. **a** Dark-field image of the mPFC at Bregma 3.20–2.70. Labeled arrows indicate the distances measured (*A*, the thickness of the mPFC at the upper end of the fmi; *B*, the thickness of the mPFC at the lower end of the fmi; *C*, the height of the fmi). **b** The thickness of the mPFC on the left- and right-hand side of the brain at the same Bregma level. **c** The height of the fmi (same Bregma level). **d** Dark-field image of the PAG at Bregma −6.8. The white line shows the region investigated. **e**. The area of the PAG as measured at Bregma −6.8. The area of the Aq was deduced. *A* the thickness of the mPFC at the upper end of the fmi, *Aq* aqueduct, *B* the thickness of the mPFC at the lower end of the fmi, *C* the height of the fmi, *Cg1* anterior cingulate, *control* socially reared rats, *DP* dorsal peduncular cortex, *DR* dorsal raphe, *fmi* forceps minor, *IL* infralimbic cortex, *PAG* periaqueductal gray, *PrL* prelimbic cortex, *PWSI* post-weaning social isolation, and *asterisk* statistically significant differences between control and PWSI rats ($p < 0.05$ at least). Note that the size of the fmi and PAG were established to asses overall changes in brain size

delineated above for cortical thickness analysis, i.e., between the upper and lower end of the forceps minor of corpus callosum, using Image J software (v1.41; http://rsbweb.nih.gov/ij/) with standardized settings across experimental subjects (Fig. 2). A background level (threshold) was obtained from each section and subtracted from measured optical density for statistical analysis.

Neuronal activation patterns: c-Fos expression in the mPFC

Sections were processed as described above. The primary antibody for c-Fos staining was sc-52 (1:5000, Santa Cruz Biotechnology) which was detected by biotinylated secondary antibodies (1:1000 in PBS with 2.5 % NHS or NGS; Jackson ImmunoResearch) and avidin–biotin complex (ABC, 1:1000; Vector Laboratories) for 1 h each at room temperature. The peroxidase reaction was developed in the presence of diaminobenzidine tetrahydrochloride (0.2 mg/ml), nickel–ammonium sulfate (0.1 %) and hydrogen peroxide (0.003 %) dissolved in Tris buffer. Microscopic images were digitized by an Olympus CCD camera using a 10× magnification lens and stained particles were counted by an experimenter blind to treatment conditions.

In the mPFC, the c-Fos signal was counted by overlaying a grid over the structure as shown in Fig. 3a. The size of individual cells within the grid was 0.01 × 0.01 mm. The grid was adjusted to the sections based on anatomical landmarks including the medial longitudinal fissure and the forceps minor of the corpus callosum. Labeled neuronal nuclei were counted separately

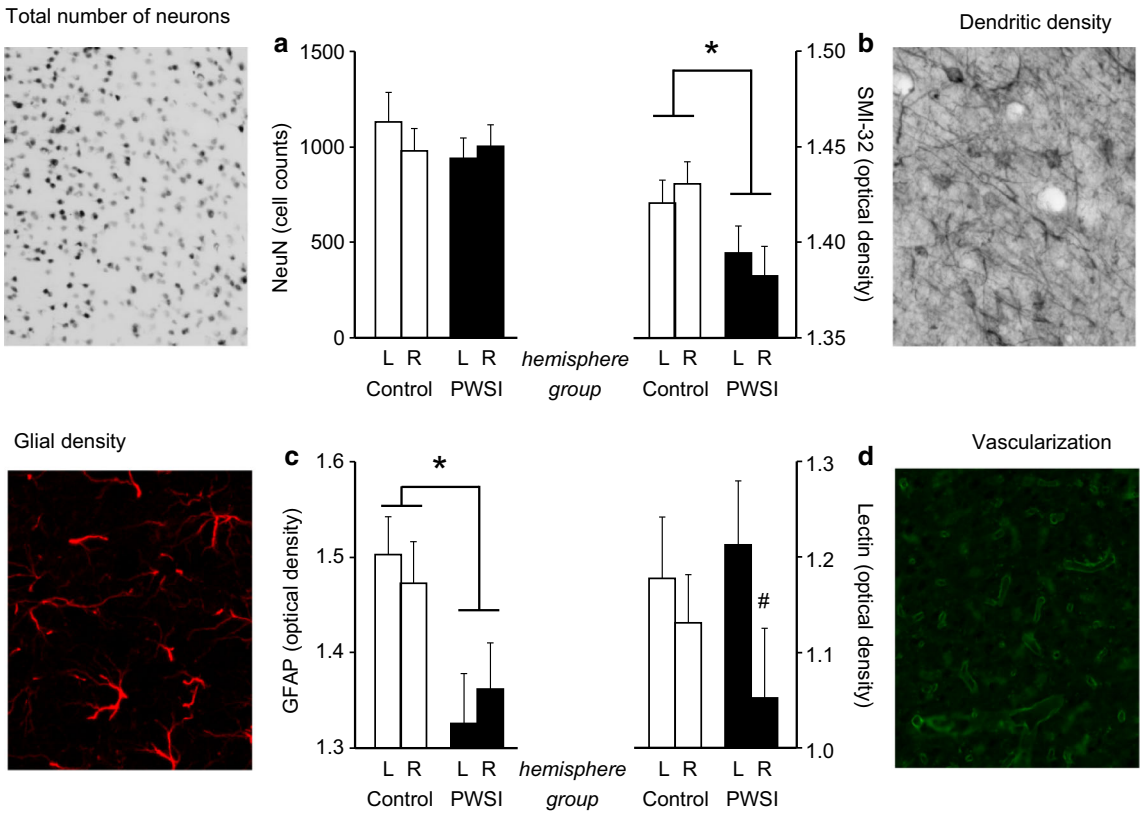

Fig. 2 Micro-structural changes in the mPFC at Bregma 3.20-2.70. **a** The number of NeuN-positive nuclei counted on one section at Bregma 3.20-2.70 within the area outlined in Fig. 3a. **b**, **c**, **d** The optical density of SMI-32, GFAP, and Lectin staining at the same Bregma level, which indicates the density of dendrites, glia cells, and micro-vessels, respectively. A representative photomicrograph of each staining was shown next to the graph. *Control* socially reared rats, *L* left-hand side of the brain, *PWSI* post-weaning social isolation, *R* right-hand side of the brain, *asterisk* significant difference between control and PWSI rats, and *hash* significant left–right differences ($p < 0.05$ at least in both cases)

for each grid, and identified based on column and row identifiers (letters and figures, respectively). To check whether differences in c-Fos expression were due to changes in neuron counts, the NeuN signal was also counted within the same grid.

Neurochemical characterization of activated neurons in the mPFC

We assessed the neurochemical characteristics of c-Fos-expressing neurons by triple labeling for c-Fos, the calcium/calmodulin-dependent protein kinase II (CaMKII), a marker of cortical glutamatergic pyramidal projection neurons (Liu and Jones 1996), and GABA, a marker of GABAergic interneurons (Menegola et al. 2008; Wolansky et al. 2007). Briefly, sections were processed as described above with minimal changes described below. After blocking with 0.1 M PB containing 10 % NGS for 30 min, sections were labeled at 4 °C with primary antibodies against c-Fos (polyclonal guinea pig, 1:5000, Cat. No. 226 004; Synaptic Systems), CaMKII (monoclonal mouse, 1:500, MA1-048; Pierce Biotechnology), and GABA (polyclonal rabbit, 1:500, A2052; Sigma-Aldrich) by 48-h incubation in 0.1 M PB solution containing 0.1 % Triton X-100 and 2 % NGS. After multiple rinsing, sections were incubated with goat anti-rabbit Alexa Fluor 594-labeled secondary antibody (1:200, Life Technologies) in TBS for overnight at 4 °C. This step was followed by 2 h incubation with secondary antibodies Alexa Fluor 488-labeled goat anti-guinea pig (1:200, Life Technologies) and Alexa Fluor 647-labeled goat anti-mouse (1:200, Life Technologies). Finally, sections were rinsed in TBS, mounted on slides, and coverslipped using Mowiol fluorescent mounting medium. Fluorescent images of infralimbic and prelimbic cortices of mPFC were studied by a C2 confocal laser scanning microscope (Nikon Europe, Amsterdam, The Netherlands). We used 488, 561 and 642 nm lasers (CVI Melles Griot), and scanning was performed in channel series mode through Plan-Apochromat VC 20x objective (with 0.75 numerical aperture). Using tile scanning, bilateral mPFC images (at Bregma 3,2 rosto-caudal level) were taken across four sections in each subject. The

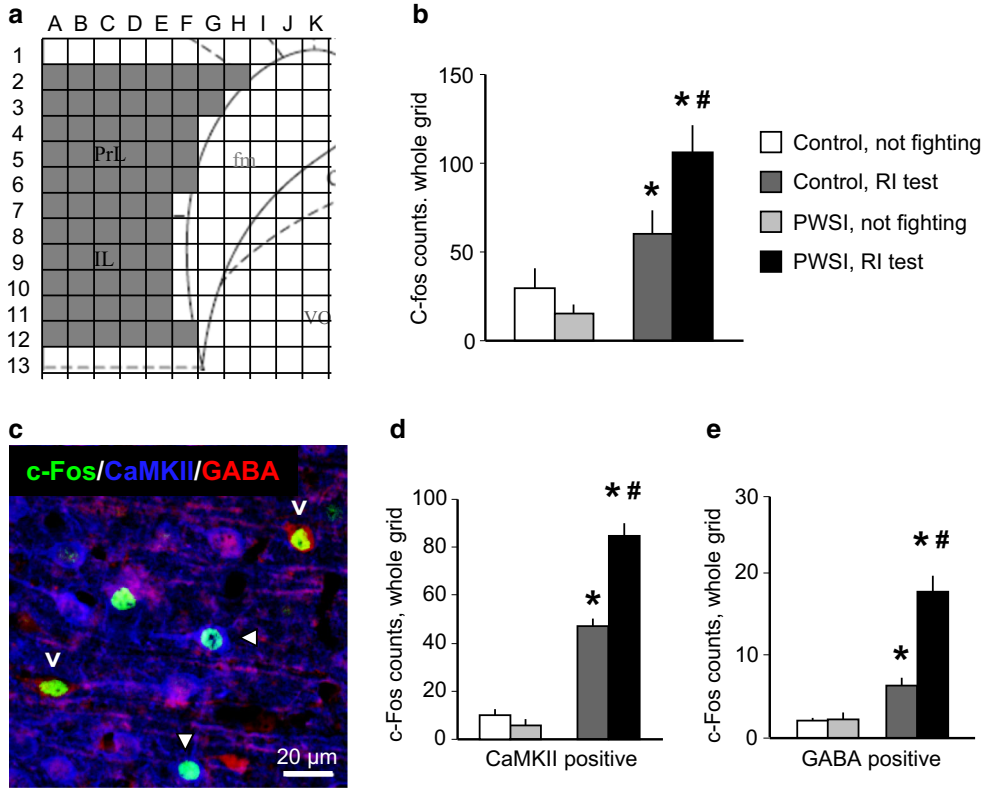

Fig. 3 The effects of PWSI and fighting on brain activation levels at Bregma 3.20-2.70. **a** The mPFC area investigated, also showing the grid overlaid over sections. The grid was adapted to each particular brain section based on anatomical landmarks. Cells within the grid were identified by column and row headings (*letters and numbers*, respectively). **b** Average number of c-Fos-labeled nuclei within the whole grid (within the *gray area* outlined in *panel a*). **c** Photomicrograph showing the triple staining for c-Fos, CaMKII and GABA. Co-localization was indicated by *arrows* (*closed arrows* CaMKII + c-Fos; *open arrows* GABA + c-Fos). Note that about 10 % of neurons were negative for both CaMKII and GABA. **d**, **e** C-fos staining in CaMKII- and GABA-expressing neurons, respectively. *Control* socially reared rats, *fm* forceps minor (see the schematic below the grid), *not fighting* not exposed to the RI test, *PWSI* post-weaning social isolation, *RI test* exposed to the resident–intruder test, *VO* ventral orbitofrontal cortex (see the schematic below the grid), *asterisk* significant effect of fighting (within rearing condition), and *hash* significant control–PWSI differences ($p < 0.05$ at least in both cases)

number of c-Fos immunopositive cells that were either CaMKII co-labeled or GABA co-labeled was quantified using NIS Elements software.

Neuronal activation patterns: c-Fos expression in other nuclei

C-Fos labeling was studied in the same brains, with sections processed and analyzed as described above. C-Fos signal was counted bilaterally in two or three sections that were 180 µm apart, and their average was considered. Section planes were standardized according to the atlas of (Paxinos and Watson 1998). A similar study was recently published (Toth et al. 2012); as such, the aim of this analysis was not the obtaining of novel information but to provide data for studying brain connectivity with special focus on the mPFC, amygdala, and hypothalamus. Brain connectivity was studied as described in the next section. We studied c-Fos activation in the central, medial, and basolateral amygdala (CeA, MeA, and BLA, respectively), which showed to have important roles in aggression control in earlier studies (Halász et al. 2002; Toth et al. 2010; Tulogdi et al. 2015), as well as in the mediobasal hypothalamus (MBH, also known as the hypothalamic attack area), and the lateral hypothalamus (LH) which have crucial roles in the elicitation of attack behavior (Kruk et al. 1983; Siegel et al. 1999; Tulogdi et al. 2010).

Mathematical modeling

We used Structural Equation Modeling (SEM) with Maximum Likelihood estimator and cluster-robust standard errors to analyze the effect of mPFC activation on the activation observed in amygdala and hypothalamic structures, and their influence on aggression. We analyzed the data using each individual grid-cell count of the mPFC as subjects. We analyzed the relationship between the different brain areas using the whole sample ($N = 45$). For

Table 1 The behavior of subjects in the resident–intruder test

Group	Biting latency	Total bite counts	Vulnerable (%)	Not signaled (%)
SR	796.3 ± 126.6	1.0 ± 0.3	8.3 ± 6.4	8.33 ± 6.4
PSWI	330.2* ± 112.9	6.85* ± 1.9	44.2* ± 6.9	23.4* ± 6.2

SR socially reared, *PSWI* post-weaning social isolation, *vulnerable* attacks targeting the head, throat, belly, or paws of opponents, *not signaled* bite initiated while engaged in non-offensive behavior (e.g., exploration, self-grooming, resting, social interaction). *Asterisk* significant effect of PWSI (see text for details). The medians (75 % confidence intervals) were as follows: biting latency, SR = 139 (335–543); biting latency, PWSI = 791 (322–566); total bites, SR = 1 (0.8–1.3); total bites, PWSI = 5 (5.9–9.5); vulnerable targets (%), SR = 0 (12.7–22.3); vulnerable targets (%), PWSI = 40 (22.2–36.9); not signaled attacks (%), SR = 0 (12.7–22.3); not signaled attacks (%), PWSI = 22.1 (18.2–29.6)

Table 2 The behavior of subjects in the second experiment, which was performed to establish the neurochemical characteristics of mPFC neurons activated by fights

Group	Biting latency	Total bite counts	Vulnerable (%)	Not signaled (%)
Controls	1027.4 ± 212.5	2.0 ± 1.0	4.0 ± 4.5	0.0 ± 0.0
PSWI	190.0* ± 36.0	5.9* ± 0.7	35.8* ± 11.6	13.9* ± 5.4
Kruskal–Wallis ANOVA	$H(1,12) = 5.54$	$H(1,12) = 5.66$	$H(1,12) = 3.97$	$H(1,12) = 3.75$
	$p < 0.02$	$p < 0.02$	$p < 0.05$	$p < 0.05$

Controls socially reared, *PSWI* post-weaning social isolation, *vulnerable* attacks targeting the head, throat, belly, or paws of opponents, *not signaled* bite initiated while engaged in non-offensive behavior (e.g., exploration, self-grooming, resting, social interaction). *Asterisk* significant effect of PWSI (see text for details)

the second model, relating brain activation and rat behavior, we used the data from the subjects with observed behavior ($N = 25$).

Statistical analyses

Data were expressed as mean ± SEM. Behavioral data were analyzed by Kruskal–Wallis ANOVA because of the non-normality of distribution. Histological data were analyzed by repeated measure ANOVA, followed by Tukey post hoc analysis when appropriate. *P* values underwent Bonferroni–Holmes correction (Holm 1979) in case of c-Fos data. When necessary, data were square-root transformed to fulfill ANOVA requirements. Significance level was set at $p < 0.05$ throughout.

Results

Resident–intruder test

As expected based on earlier studies, PWSI increased aggression in quantitative terms, and also induced the expression of deviant forms of aggression (Table 1). Rats submitted to the model started attacks sooner and delivered more biting attacks than SR rats in the resident/intruder test [$H(1,23) = 7.58$, $p < 0.01$, $H(1,23) = 8.76$, $p < 0.01$, respectively]. They also exhibited more attacks on vulnerable targets [$H(1,23) = 10.19$, $p < 0.01$], and were less prone to signal their attacks by offensive threats [$H(1,23) = 6.80$, $p < 0.01$]. Rats submitted to the second experiment behaved in a highly similar way (Table 2).

Structural alterations in the mPFC

The thickness of the mPFC was significantly reduced by PWSI at both the upper and lower end of the forceps minor in the right hemisphere [thickness at the dorsal end of forceps minor (*A*): $F_{\text{group} \times \text{brain side}}(1,28) = 10.04$; $p < 0.01$; thickness at the ventral end of forceps minor (*B*): $F_{\text{group} \times \text{brain side}}(1,28) = 8.17$; $p < 0.01$; Fig. 1]. Reduction was around 15 % in both cases. The dorsoventral extension of the forceps minor did not change significantly [$F_{\text{group}}(1,28) < 1$, $p > 0.45$; $F_{\text{group} \times \text{brain side}}(1,28) = 1.11$; $p > 0.30$; Fig. 1, distance C]. The size of the PAG did not change either [$F_{\text{group}}(1,25) < 1$, $p > 0.57$; Fig. 1c, d], suggesting that the thinning of the mPFC was not due to an overall reduction in brain size.

Despite the thinning of the right mPFC, the total number of neurons in the whole area was not altered on either side as shown by NeuN staining [$F_{\text{group}}(1,42) < 1$, $p > 0.60$; $F_{\text{brain side}}(1,42) < 1$, $p > 0.65$; $F_{\text{group} \times \text{brain side}}(1,42) = 1.36$, $p > 0.25$; Fig. 2a]. By contrast, dendritic density indexed by SMI-32 staining was reduced bilaterally in PWSI rats [$F_{\text{group}}(1,21) = 7.55$, $p < 0.05$; $F_{\text{brain side}}(1,21) < 1$, $p > 0.75$; $F_{\text{group} \times \text{brain side}}(1,21) < 1$, $p > 0.61$; Fig. 2b]. A similar decrease was observed in glial cell counts as indexed by reduced GFAP density in both hemispheres [$F_{\text{group}}(1,20) = 10.10$, $p < 0.01$; $F_{\text{brain side}}(1,20) < 1$, $p > 0.62$; $F_{\text{group} \times \text{brain side}}(1,20) = 2.37$, $p > 0.14$;

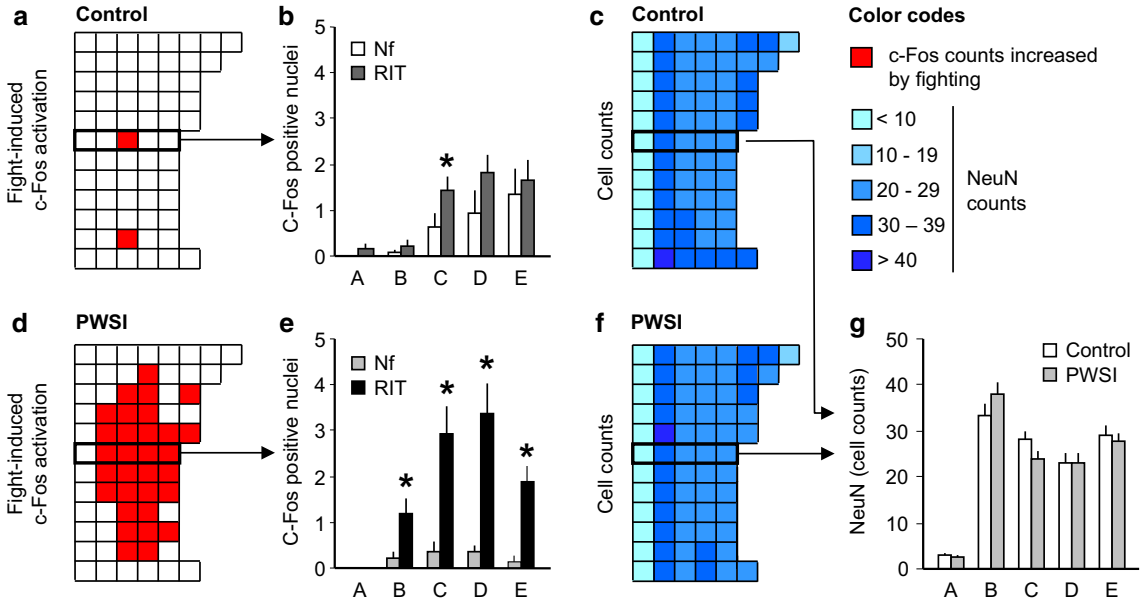

Fig. 4 Voxel-like representation of c-Fos activation within the mPFC area investigated (Bregma 3.20-2.70). The grids shown in this figure are identical with the one outlined in Fig. 3a. **a** Differences between rats exposed and not exposed to the resident–intruder test in the control group. Row 7 was outlined by a thick frame to show the region chosen for illustration in panel *b*. **b** Graph illustrating the difference between fighting and not fighting control rats at row 7 of the grid. **c** Neuron numbers in control rats within the cells of the grid as shown by NeuN staining. **d** Differences between rats exposed and not exposed to the resident–intruder test in the PWSI group. Row 7 was outlined by a thick frame to show the region chosen for illustration in panel *e*. **e** Graph illustrating the difference between fighting and not fighting PWSI rats at row 7 of the grid. **f** Neuron numbers in PWSI rats within the cells of the grid as shown by NeuN staining. **g** Graph illustrating group differences in neuron counts at row 7 of the grid (this row was outlined in graphs *c* and *f*). *Control* socially reared rats, *Nf* not exposed to RIT (not fighting), *PWSI* post-weaning social isolation, *RIT* exposed to the resident–intruder test, and *asterisk* significant effect of fighting ($p < 0.05$ at least)

Fig. 2c]. The vascularization of the investigated mPFC area was also reduced by PSWI specifically on the right-hand side of the brain as shown by reduced staining for lectin [$F_{\text{group} \times \text{brain side}}(1,26) = 4.79$; Fig. 2d].

mPFC activation in the entire mPFC

When the whole area covered by the grid shown in Fig. 3a was considered, c-Fos counts depended on the interaction between housing and fighting, i.e., exposure to the resident–intruder test [$F_{\text{housing} \times \text{fighting}}(1,54) = 9.69$; $p < 0.01$] but not on brain side. The latter factor did not provide significant differences neither alone nor in interaction with other factors (F values were between 0.08 and 0.26; corresponding p values were between 0.91 and 0.61). Exposure to the resident–intruder test increased c-Fos counts in both SR and PSWI rats, but the increase was larger in the latter group (Fig. 3b).

In the second study performed for the neurochemical identification of activated mPFC neurons, c-Fos counts were increased by fights [$F_{\text{fighting}}(1;\ 15) = 48.89$; $p < 0.01$], and was further increased by PWSI [$F_{\text{interaction}}(1;\ 15) = 10.59$; $p < 0.01$]. Surprisingly, similar situation was observed when CaMKII-expressing and GABA-expressing neurons were considered separately [$F_{\text{interaction}}(1;\ 15) = 21.67$; $p < 0.01$ and $F_{\text{interaction}}(1;\ 15) = 11.43$; $p < 0.01$, respectively]. Fights increased the number of activated glutamatergic and GABAergic neurons in controls, and activation was significantly higher in PWSI rats (Fig. 3c–e).

The voxel-like analysis of mPFC activation

In grid-based comparisons, c-Fos counts depended on the interaction between group and cell [$F_{\text{interaction}}(189, 3648) = 2.29$; $p < 0.001$], but again not on the hemisphere. In SR rats, few differences between controls and fighting rats survived Bonferroni–Holmes corrections; in fact, fighting animals showed significantly higher c-Fos counts only in cells C7 and C11 as compared to the corresponding cells of non-fighting controls (Fig. 4a). This suggests that the overall increase shown in Fig. 3b was distributed relatively uniformly over the whole area, without outstanding increases in particular sub-regions. By contrast, grid-based comparisons revealed the activation of a clearly circumscribable area in PWSI rats. The area roughly corresponds to neuron layers 3 and 5–6, covers both the PrL and IL, but does not entirely stretch over their dorsoventral extension (Fig. 4d). The magnitude of differences is illustrated by c-Fos counts shown for row 7

Table 3 C- Fos activation patterns in brain areas studied by structural equation modeling

Group	CeA ± SEM	MeA ± SEM	BLA ± SEM	AMYtot ± SEM	MBH ± SEM	LH ± SEM	*N*
SR–control	11.68 ± 1.79	13.14 ± 2.39	9.67 ± 1.93	11.50 ± 1.48	11.93 ± 2.27	17.23 ± 3.93	10
SR–RI test	28.00* ± 3.67	71.16* ± 9.52	45.00* ± 8.22	48.06* ± 6.97	32.35* ± 3.75	34.52* ± 3.96	10
PWSI–control	14.01 ± 3.02	15.62 ± 3.59	9.30 ± 2.12	12.98 ± 2.42	10.28 ± 1.81	14.40 ± 3.84	12
PWSI–RI test	29.05* ± 3.51	107.04*$^{\#}$ ± 10.36	63.45* ± 8.92	66.51*$^{\#}$ ± 7.00	39.08* ± 3.90	40.68* ± 3.98	13
$F_{\text{rearing}}(1,41)$	0.28	6.18	1.92	3.48	0.65	0.18	45
$p<$	0.6	0.02	0.2	0.07	0.4	0.7	
$F_{\text{fighting}}(1,41)$	24.23	93.78	46.93	71.12	60.69	29.92	
$p<$	0.0001	0.0001	0.0001	0.0001	0.0001	0.0001	
$F_{\text{interaction}}(1,41)$	0.04	4.68	2.07	2.52	1.76	1.28	
$p<$	0.8	0.04	0.2	0.1	0.2	0.3	

In an earlier study that investigated aggression-induced brain activation patterns in PWSI rats, the same nuclei were investigated in a more detailed way, e.g., by dividing the nuclei rostrocaudally (Toth et al. 2012). Albeit no similar distinctions were employed here, the two studies provided rather similar findings. *SR* socially reared, *PWSI* post-weaning social isolation, *RI* resident–intruder test, *CeA* central amygdala, *MeA* medial amygdala, *BLA* basolateral amygdala, *AMYtot* average of CeA, Mea, BLA, *MBH* mediobasal hypothalamus (hypothalamic attack area), *LH* lateral hypothalamus, *asterisk* significant effect of fighting (control vs. fighting), *hash* significant difference between SR–RI test and PWSI–RI test ($p < 0.05$ at least after Bonferroni–Holmes correction in both cases)

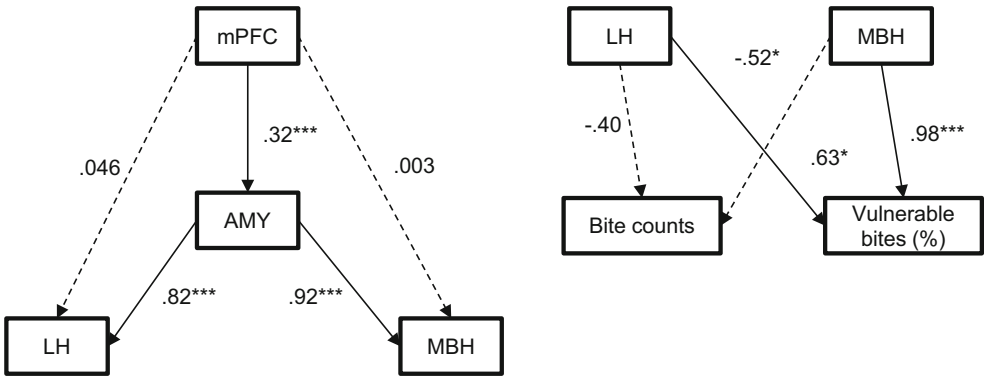

Fig. 5 Structural Equation Model for the brain activation analysis. *AMY*, c-Fos counts averaged for the amygdala sub-regions investigated (see Table 2); *LH* c-Fos counts within the lateral hypothalamus, *MBH* c-Fos counts within the mediobasal hypothalamus, *mPFC* average c-Fos counts within the grid outlined in Fig. 3a; *displayed path values* standardized path coefficients, *asterisk* significant connections ($p < 0.001$). Note that similar path coefficients were obtained with amygdala sub-regions; therefore, the whole amygdala is shown in this graph

(cells A7-E7) in SR and PWSI rats (Fig. 4b, e, respectively). To investigate whether changes in c-Fos expression were associated with changes in neuron numbers, the NeuN signal was counted using a grid similar to that used to study c-Fos activation. Neuron counts depended on the interaction between social background and cell [$F_{\text{interaction}}(63, 1152) = 1.37$; $p < 0.05$]. However, no group differences were observed at any of the grid cells (Fig. 4c, f). The significant interaction resulted from group-specific relations between different cells of the grid. For instance, NeuN counts in grid cells C6 and C12 were significantly different in SR rats (C6 vs.C12: $p < 0.05$), whereas the same cells did not differ in PWSI rats (C6 vs.C12: $p > 0.1$). While such findings are potentially interesting, no significant SR–PWSI differences were observed when the same cells were compared. For instance, group differences were seen neither in cell C6 (SR vs. PWSI, $p = 0.2$) nor in cell C12 (SR vs. PWSI, $p > 0.8$). The similarity of cell counts is illustrated for row 7 (cells A7-E7) in Fig. 4g.

Taken together, these findings show that the activation of the mPFC was larger in PWSI rats, and the increase in activation was restricted to a sub-region of the area. Differences in activation patterns were not secondary to differences in neuron counts.

The expression of the activation marker c-Fos in the amygdala and hypothalamus

c-Fos expression analysis was performed for the assessment of the effects of PWSI on neuronal activation within selected regions of the amygdala and hypothalamus under basal conditions and after fighting. The data of this analysis

are shown in Table 3. Overall, no differences were found between SR and PWSI rats at baseline. Fighting (exposure to the resident–intruder test) increased c-Fos activation in both groups, in all the five investigated areas. Fight-induced activation was higher in the medial amygdala of PWSI rats as compared to SR rats. A similar trend was observed at the level of the whole amygdala. These findings are essentially similar to those published earlier (Toth et al. 2012), and were established to study brain connectivity.

Brain connectivity: structural equation modeling

To evaluate whether neuronal co-activation in different brain regions can explain different aggressive behaviors, we performed SEM analyses based on anatomical evidence for connectivity and correlational analyses between c-Fos counting in different brain areas. First, we found that a fully saturated cluster SEM model showed no significant direct relationships between c-Fos counts in the prefrontal cortex (the area depicted in Figs. 1a, 3a) and those observed in the LH and MBH. There was, however, a significant mediating effect of amygdala on both LH and MBH. Higher prefrontal activation (higher c-Fos counts) led to higher amygdala activation ($\beta = 0.32$, $p < 0.001$), and amygdala activation was strongly associated with higher c-Fos counts both in the LH ($\beta = 0.82$, $p < 0.001$) and MBH ($\beta = 0.92$, $p < 0.001$) (Fig. 5a). Noteworthy, similar findings were obtained when the three amygdala sub-regions were considered separately; therefore, we presented in Fig. 5 calculi based on total amygdala c-Fos counts (depicted in Table 3 as AMYtot).

For behavioral measures, because of the highly uneven distribution, the dependent variables (bites and vulnerable attacks) were transformed into categorical variables based on quintiles which represent degrees of aggressive behavior. A structural equation model, including only the sample with observed behavior, shows a significant effect of both LH and MBH activation on vulnerable attack bites (LH: $\beta = -0.52$, $p < 0.05$, MBH: $\beta = 0.98$, $p < 0.05$). Only MBH activation was significantly, and positively associated with regular bites ($\beta = 0.63$, $p < 0.05$) (Fig. 5b).

Discussion

Main findings

Post-weaning social isolation led to the development of escalated aggression in adulthood as shown by all three increased attack counts, increased share of bites directed towards vulnerable body parts of opponents and reduced social signaling of attacks. Effects were highly reproducible. These deviations from species-typical behavioral characteristics were associated with significant reduction in the thickness of the right medial prefrontal cortex. Changes seemed specific to this brain region as, for example, the size of the forceps minor and PAG did not change. We also observed a bilateral decrease in dendritic and glial density, and reduced vascularization on the right-hand side of the same region. Despite the above-mentioned structural deficits, aggressive encounters enhanced the activation of the prefrontal cortex in PWSI rats as compared to controls. A voxel-like functional analysis revealed that overactivation was restricted to a circumscribed sub-region of the mPFC.

Our present findings support the notion that escalated aggression develops on the background of disturbed prefrontal development, fitting the general view that prefrontal deficits promote aggressiveness; moreover, according to the literature, those deficits may underlie aggression-related psychopathologies (Siever 2008; Blair 2010). At the same time, however, chronic prefrontal deficits are associated with increased abnormal fight-induced activation in a distinct prefrontal sub-region, which cannot be explained based on this theory. Importantly, both glutamatergic and GABAergic neurons were overactivated, which precludes the possibility that mPFC activation resulted from the unilateral increase in the activity of local inhibitory circuits.

Structural mPFC deficits and aggression

Early stress-induced changes in prefrontal volume or cortical thickness have not been associated with aggression in animals so far. Earlier studies focused on the role of such deficits in schizophrenia-like symptoms, e.g., deficits in prepulse inhibition, impulsivity, and locomotor hyperactivity (Day-Wilson et al. 2006; Schubert et al. 2009). In these studies, post-weaning social isolation reduced prefrontal cortex thickness or volume by 6–7 %, which is smaller, but comparable with the reduction observed by us ($\sim$15 %). By contrast, volume reductions were readily observed in humans showing aggression-related psychopathologies; moreover, the extent of reduction (11–24 % depending on the study) was similar to that observed in our rats and, in addition, changes were usually also observed in the right hemisphere (antisocial personality disorder Raine et al. 2000; borderline personality disorder, Tebartz van Elst et al. 2003; childhood disruptive behavior, Fahim et al. 2011; psychopathy, Boccardi et al. 2011). In our study, the total number of neurons was not affected by post-weaning social isolation, despite size differences in the investigated prefrontal area. Albeit this may seem somewhat surprising, similar findings were reported earlier, e.g., both experimental hypothyroidism

and post-weaning social isolation reduced the size of the prefrontal cortex while neuron counts increased or remained unchanged, respectively (Madeira et al. 1990; Day-Wilson et al. 2006). In these cases, size reductions were attributed to neuropil impoverishment. It was also repeatedly shown that early stressors reduce glia counts and dendritic density in the medial prefrontal cortex. Such findings were perceived as mechanistically relevant for the development of anxiety, depression, or schizophrenia (Pascual and Zamora-Leon 2007; Wang et al. 2012; Skupio et al. 2015). By contrast, an early stressor-induced reduction in vascularization was not reported earlier in rodents, but prefrontal reductions in blood flow and glucose metabolism—likely consequences of decreased vascularization—are common in aggression-related psychopathologies (Hirono et al. 2000; Goethals et al. 2005).

Taken together, our findings show that post-weaning social isolation induces a complex array of structural deficits in the medial prefrontal cortex. Similar deficits were observed in rodents submitted to early stressors but this is the first rodent study that links such changes to aggressive behavior. Notably, similar deficits were observed in humans suffering from aggression-related psychopathologies.

Prefrontal activation and aggression

Aggression increases prefrontal activity in both humans and rodents (Lotze et al. 2007; Halasz et al. 2006); moreover, a further increase in activation was reported in animal models of escalated aggression (Haller et al. 2006; Beiderbeck et al. 2012; Toth et al. 2012) and aggression-related psychopathologies (Herpertz and Sass 2000; Schneider et al. 2000; Veit et al. 2010; Vollm et al. 2010). The voxel-like approach employed here refined these earlier observations by showing that activation is restricted to a distinct sub-area of the mPFC, which encompasses both the PrL and IL, but does not cover their entire extension. Interestingly, this subregion overlaps with the area, which contains mPFC neurons directly projecting to the mediobasal hypothalamus (Toth et al. 2010), which indirectly suggests a role for this projection in the control aggression in general, and in its abnormal manifestations in particular. While these findings are in line with rodent and human data as regards the activation of the mPFC by aggression in general and its overactivation in models of abnormal aggression, they question the general aggression-inhibitory role of the PFC suggesting that the theory needs adjustments.

mPFC: amygdala interactions in aggression

A bidirectional mPFC–amygdala connection plays a pivotal role in emotionally salient information processing and social evaluation in both rodents and humans (Davidson et al. 2000; Milad et al. 2006; Kim et al. 2011; Kumar et al. 2014). However, the role of this connection in aggression control was studied so far in humans only, where reduced PFC–amygdala connectivity was observed in antisocial personality disorder and psychopathy (Motzkin et al. 2011; Hoppenbrouwers et al. 2013; Contreras-Rodriguez et al. 2015; Wolf et al. 2015). Our findings are the first to indicate that enhanced functional connectivity in the mPFC–amygdala network is involved in the control of rodent abnormal aggression as shown by the findings of the SEM analysis. An interesting aspect of our findings is that antisocial personality disorder and psychopathy are mainly associated with instrumental/proactive forms of aggression, whereas the PWSI paradigm models emotional/reactive aggression (Haller et al. 2014). Tentatively, this suggests that enhanced mPFC–amygdala connectivity subserves abnormal manifestations of aggression depending on its type (reactive or proactive).

Dual control of aggression by the mPFC

The main finding of this study is that PSWI interferes with prefrontal development, and results in multiple structural deficits in this area, but at the same time the mPFC is overactivated by aggressive encounters in rats submitted to PSWI.

The relevance of prefrontal deficits for aggression control can easily be deduced from earlier studies performed in either rodents or humans. In the latter, prefrontal deficits were associated with psychological features, which escalate aggressiveness, particularly with poor cognitive control over behavior, punishment resistance, predilection towards rule braking, and increases in anger and impulsiveness (Deckel et al. 1996; Dinn and Harris 2000; Potts et al. 2006; Spitzer et al. 2007; Arnsten and Rubia 2012; Fulwiler et al. 2012). Similar interactions between prefrontal and emotional/cognitive deficits were observed in animals (Dalley et al. 2002; Sagvolden 2006; Chudasama et al. 2012; Paine et al. 2013; Bicks et al. 2015), suggesting a causal link between prefrontal deficits observed in PWSI rats and their aggressiveness. This assumption supports the "prefrontal deficit theory" of aggression.

Aggression-enhanced mPFC activation is more difficult to interpret. Several alternative working hypotheses can be proposed:

1. mPFC overactivation could, in fact, limit aggression if interpreted in terms of a negative feedback mechanism. Such a rebound effect may be stronger if aggression was expressed at higher levels, which may explain differences between PSWI and socially reared rodents. However, visual and perceptual challenges by physically inaccessible opponents also increase prefrontal

activation in the absence of aggressive behavior, i.e., when there is no aggression to be "stopped" by the mPFC (Halasz et al. 2006; Ferris et al. 2008; Ago et al. 2013). This decreases the plausibility of the explanation. The study by Takahashi et al. (2014) ostensibly still supports the assumption, as these authors showed that the optogenetic stimulation of the "mPFC" in resident–intruder tests decreases aggression. In their study, however, the target of optogenetic stimulation is unclear. The schematics that depict the site of stimulation (Takahashi et al. (2014): Fig. 1d, and the left-hand panel of Fig. 5) show the mouse brain at Bregma 2.2 mm (Paxinos and Franklin 2001). In contrast to rats, the medial orbitofrontal cortex (MO) is situated beneath the PrL at this level in mice, and the schematics suggest that optic stimulation targeted primarily the MO. As such, the findings of this study remain unclear at present.

2. mPFC activation may have been unrelated to aggression control, and either resulted from disorganized prefrontal functioning or reflected emotional processes. While this assumption cannot be ruled out, our SEM analyses identified clear associations between prefrontal activation and the functioning of hypothalamic centers involved in the control of biting attacks. In addition, the mPFC sub-region which was overactivated by fights contains neurons that project directly to the MBH (Toth et al. 2010). These two arguments make this assumption somewhat unlikely.
3. One can assume that the mPFC, particularly the sub-region identified by this study promotes the expression of aggression by its subcortical projections. This may be exerted either by the inhibition of subcortical GABAergic neurons by long-ranging GABAergic projections—disinhibition by the inhibition of inhibition; Potegal (2012)—or by the direct stimulation of subcortical areas involved in the initiation and maintenance of attacks.
4. (iv) Finally, the mPFC may coordinate the movements that make up a biting attack or may control the choice of behavioral responses given to the actions of partners. This assumption is based on recent hypotheses on the role of the prefrontal cortex in the selection, preparation, and execution of movements in both humans and rodents (Badre and D'Esposito 2009; Balleine and O'Doherty 2010; Chudasama et al. 2012). In brief, the mPFC may affect aggressive behavior by functionally coupling motor and cognitive functions.

Information available at present is insufficient for definitive statements, but circumstantial evidence suggests that last two assumptions are more likely than the first two.

Concluding remarks

Taken together, our findings may help resolving contradictory structural and functional findings as it regards the role of the mPFC in aggression control. On one hand, we showed that—similar to humans—early stress-induced structural deficits of the mPFC are associated with heightened and abnormal forms of aggression in rodents. We also showed that structural deficits do not simply result in loss of functions, but are marked by enhanced fight-induced activation of the mPFC in adulthood. This phenomenon requires further studies with regard to their underlying mechanisms and functional interpretation. Overall, our findings indicate that the prefrontal control of aggression cannot be solely explained by inhibitory mechanisms; understanding requires more complex approaches.

Acknowledgments Funding for this study was provided by National Research, Development and Innovation Office Fund (NKFI) Grant No. 112907.

Compliance with ethical standards

Conflict of interest The authors declare that they have no conflict of interest.

References

Ago Y, Araki R, Tanaka T, Sasaga A, Nishiyama S, Takuma K, Matsuda T (2013) Role of social encounter-induced activation of prefrontal serotonergic systems in the abnormal behaviors of isolation-reared mice. Neuropsychopharmacology 38(8):1535–1547. doi:10.1038/npp.2013.52

Aksic M, Radonjic NV, Aleksic D, Jevtic G, Markovic B, Petronijevic N, Radonjic V, Filipovic B (2013) Long-term effects of the maternal deprivation on the volume and number of neurons in the rat neocortex and hippocampus. Acta Neurobiol Exp 73(3):394–403

Arnsten AF, Rubia K (2012) Neurobiological circuits regulating attention, cognitive control, motivation, and emotion: disruptions in neurodevelopmental psychiatric disorders. J Am Acad Child Adolesc Psychiatry 51(4):356–367. doi:10.1016/j.jaac.2012.01.008

Badre D, D'Esposito M (2009) Is the rostro-caudal axis of the frontal lobe hierarchical? Nat Rev Neurosci 10(9):659–669. doi:10.1038/nrn2667

Balleine BW, O'Doherty JP (2010) Human and rodent homologies in action control: corticostriatal determinants of goal-directed and habitual action. Neuropsychopharmacology 35(1):48–69. doi:10.1038/npp.2009.131

Beiderbeck DI, Reber SO, Havasi A, Bredewold R, Veenema AH, Neumann ID (2012) High and abnormal forms of aggression in rats with extremes in trait anxiety–involvement of the dopamine system in the nucleus accumbens. Psychoneuroendocrinology 37(12):1969–1980. doi:10.1016/j.psyneuen.2012.04.011

Bicks LK, Koike H, Akbarian S, Morishita H (2015) Prefrontal Cortex and Social Cognition in Mouse and Man. Front Psychol 6:1805. doi:10.3389/fpsyg.2015.01805

Blair RJ (2010) Psychopathy, frustration, and reactive aggression: the role of ventromedial prefrontal cortex. Br J Psychol (London, England: 1953) 101(Pt 3):383–399. doi:10.1348/000712609x418480

Blair RJ (2015) Psychopathic traits from an RDoC perspective. Curr Opin Neurobiol 30:79–84. doi:10.1016/j.conb.2014.09.011

Boccardi M, Frisoni GB, Hare RD, Cavedo E, Najt P, Pievani M, Rasser PE, Laakso MP, Aronen HJ, Repo-Tiihonen E, Vaurio O, Thompson PM, Tiihonen J (2011) Cortex and amygdala morphology in psychopathy. Psychiatry Res 193(2):85–92. doi:10.1016/j.pscychresns.2010.12.013

Carre JM, Murphy KR, Hariri AR (2013) What lies beneath the face of aggression? Social Cognit Affect Neurosci 8(2):224–229. doi:10.1093/scan/nsr096

Chudasama Y, Doobay VM, Liu Y (2012) Hippocampal-prefrontal cortical circuit mediates inhibitory response control in the rat. J Neurosci Off J Soc Neurosci 32(32):10915–10924. doi:10.1523/jneurosci.1463-12.2012

Contreras-Rodriguez O, Pujol J, Batalla I, Harrison BJ, Soriano-Mas C, Deus J, Lopez-Sola M, Macia D, Pera V, Hernandez-Ribas R, Pifarre J, Menchon JM, Cardoner N (2015) Functional connectivity bias in the prefrontal cortex of psychopaths. Biol Psychiatry 78(9):647–655. doi:10.1016/j.biopsych.2014.03.007

Dalley JW, Theobald DE, Pereira EA, Li PM, Robbins TW (2002) Specific abnormalities in serotonin release in the prefrontal cortex of isolation-reared rats measured during behavioural performance of a task assessing visuospatial attention and impulsivity. Psychopharmacology 164(3):329–340. doi:10.1007/s00213-002-1215-y

Davidson RJ, Putnam KM, Larson CL (2000) Dysfunction in the neural circuitry of emotion regulation–a possible prelude to violence. Science 289(5479):591–594

Day-Wilson KM, Jones DN, Southam E, Cilia J, Totterdell S (2006) Medial prefrontal cortex volume loss in rats with isolation rearing-induced deficits in prepulse inhibition of acoustic startle. Neuroscience 141(3):1113–1121. doi:10.1016/j.neuroscience.2006.04.048

Decety J, Porges EC (2011) Imagining being the agent of actions that carry different moral consequences: an fMRI study. Neuropsychologia 49(11):2994–3001. doi:10.1016/j.neuropsychologia.2011.06.024

Deckel AW, Hesselbrock V, Bauer L (1996) Antisocial personality disorder, childhood delinquency, and frontal brain functioning: EEG and neuropsychological findings. J Clin Psychol 52(6):639–650. doi:10.1002/(sici)1097-4679(199611)52:6<639:aid-jclp6>3.0.co;2-f

Dinn WM, Harris CL (2000) Neurocognitive function in antisocial personality disorder. Psychiatry Res 97(2–3):173–190

Ermer E, Cope LM, Nyalakanti PK, Calhoun VD, Kiehl KA (2013) Aberrant paralimbic gray matter in incarcerated male adolescents with psychopathic traits. J Am Acad Child Adoles Psychiatry 52(1):94–103 e103. doi:10.1016/j.jaac.2012.10.013

Fahim C, He Y, Yoon U, Chen J, Evans A, Perusse D (2011) Neuroanatomy of childhood disruptive behavior disorders. Aggress Behav 37(4):326–337. doi:10.1002/ab.20396

Ferris CF, Stolberg T, Kulkarni P, Murugavel M, Blanchard R, Blanchard DC, Febo M, Brevard M, Simon NG (2008) Imaging the neural circuitry and chemical control of aggressive motivation. BMC Neurosci 9:111. doi:10.1186/1471-2202-9-111

Fulwiler CE, King JA, Zhang N (2012) Amygdala-orbitofrontal resting-state functional connectivity is associated with trait anger. NeuroReport 23(10):606–610. doi:10.1097/WNR.0b013e3283551cfc

Gilbert R, Widom CS, Browne K, Fergusson D, Webb E, Janson S (2009) Burden and consequences of child maltreatment in high-income countries. Lancet (London, England) 373(9657):68–81. doi:10.1016/s0140-6736(08)61706-7

Glenn AL, Johnson AK, Raine A (2013) Antisocial personality disorder: a current review. Curr Psychiatry Rep 15(12):427. doi:10.1007/s11920-013-0427-7

Goethals I, Audenaert K, Jacobs F, Van den Eynde F, Bernagie K, Kolindou A, Vervaet M, Dierckx R, Van Heeringen C (2005) Brain perfusion SPECT in impulsivity-related personality disorders. Behav Brain Res 157(1):187–192. doi:10.1016/j.bbr.2004.06.022

Halasz J, Toth M, Kallo I, Liposits Z, Haller J (2006) The activation of prefrontal cortical neurons in aggression–a double labeling study. Behav Brain Res 175(1):166–175. doi:10.1016/j.bbr.2006.08.019

Halász J, Liposits Z, Kruk MR, Haller J (2002) Neural background of glucocorticoid dysfunction-induced abnormal aggression in rats: involvement of fear- and stress-related structures. Eur J Neurosci 15(3):561–569

Haller J, Toth M, Halasz J, De Boer SF (2006) Patterns of violent aggression-induced brain c-fos expression in male mice selected for aggressiveness. Physiol Behav 88(1–2):173–182. doi:10.1016/j.physbeh.2006.03.030

Haller J, Harold G, Sandi C, Neumann ID (2014) Effects of adverse early-life events on aggression and anti-social behaviours in animals and humans. J Neuroendocrinol 26(10):724–738. doi:10.1111/jne.12182

Hermans EJ, Ramsey NF, van Honk J (2008) Exogenous testosterone enhances responsiveness to social threat in the neural circuitry of social aggression in humans. Biol Psychiatry 63(3):263–270. doi:10.1016/j.biopsych.2007.05.013

Herpertz SC, Sass H (2000) Emotional deficiency and psychopathy. Behav Sci Law 18(5):567–580

Hirono N, Mega MS, Dinov ID, Mishkin F, Cummings JL (2000) Left frontotemporal hypoperfusion is associated with aggression in patients with dementia. Arch Neurol 57(6):861–866

Holm S (1979) A simple sequentially rejective multiple test procedure. Scand J Stat 6:65–70

Hoppenbrouwers SS, Nazeri A, de Jesus DR, Stirpe T, Felsky D, Schutter DJ, Daskalakis ZJ, Voineskos AN (2013) White matter deficits in psychopathic offenders and correlation with factor structure. PLoS One 8(8):e72375. doi:10.1371/journal.pone.0072375

Kim MJ, Loucks RA, Palmer AL, Brown AC, Solomon KM, Marchante AN, Whalen PJ (2011) The structural and functional connectivity of the amygdala: from normal emotion to pathological anxiety. Behav Brain Res 223(2):403–410. doi:10.1016/j.bbr.2011.04.025

Kruk MR, Van der Poel AM, Meelis W, Hermans J, Mostert PG, Mos J, Lohman AH (1983) Discriminant analysis of the localization of aggression-inducing electrode placements in the hypothalamus of male rats. Brain Res 260(1):61–79

Kumar S, Hultman R, Hughes D, Michel N, Katz BM, Dzirasa K (2014) Prefrontal cortex reactivity underlies trait vulnerability to chronic social defeat stress. Nature Commun 5:4537. doi:10.1038/ncomms5537

Liu XB, Jones EG (1996) Localization of alpha type II calcium calmodulin-dependent protein kinase at glutamatergic but not gamma-aminobutyric acid (GABAergic) synapses in thalamus and cerebral cortex. Proc Natl Acad Sci USA 93(14):7332–7336

Lotze M, Veit R, Anders S, Birbaumer N (2007) Evidence for a different role of the ventral and dorsal medial prefrontal cortex for social reactive aggression: an interactive fMRI study. Neuroimage 34(1):470–478. doi:10.1016/j.neuroimage.2006.09.028

Madeira MD, Pereira A, Cadete-Leite A, Paula-Barbosa MM (1990) Estimates of volumes and pyramidal cell numbers in the prelimbic subarea of the prefrontal cortex in experimental hypothyroid rats. J Anat 171:41–56

Marquez C, Poirier GL, Cordero MI, Larsen MH, Groner A, Marquis J, Magistretti PJ, Trono D, Sandi C (2013) Peripuberty stress leads to abnormal aggression, altered amygdala and orbitofrontal reactivity and increased prefrontal MAOA gene expression. Translational psychiatry 3:e216. doi:10.1038/tp.2012.144

Menegola M, Misonou H, Vacher H, Trimmer JS (2008) Dendritic A-type potassium channel subunit expression in CA1 hippocampal interneurons. Neuroscience 154(3):953–964

Miczek KA, de Boer SF, Haller J (2013) Excessive aggression as model of violence: a critical evaluation of current preclinical methods. Psychopharmacology 226(3):445–458. doi:10.1007/s00213-013-3008-x

Milad MR, Rauch SL, Pitman RK, Quirk GJ (2006) Fear extinction in rats: implications for human brain imaging and anxiety disorders. Biol Psychol 73(1):61–71. doi:10.1016/j.biopsycho.2006.01.008

Montag C, Weber B, Trautner P, Newport B, Markett S, Walter NT, Felten A, Reuter M (2012) Does excessive play of violent first-person-shooter-video-games dampen brain activity in response to emotional stimuli? Biol Psychol 89(1):107–111. doi:10.1016/j.biopsycho.2011.09.014

Motzkin JC, Newman JP, Kiehl KA, Koenigs M (2011) Reduced prefrontal connectivity in psychopathy. J Neurosci Off J Soc Neurosci 31(48):17348–17357. doi:10.1523/jneurosci.4215-11.2011

New AS, Hazlett EA, Newmark RE, Zhang J, Triebwasser J, Meyerson D, Lazarus S, Trisdorfer R, Goldstein KE, Goodman M, Koenigsberg HW, Flory JD, Siever LJ, Buchsbaum MS (2009) Laboratory induced aggression: a positron emission tomography study of aggressive individuals with borderline personality disorder. Biol Psychiatry 66(12):1107–1114. doi:10.1016/j.biopsych.2009.07.015

Paine TA, Asinof SK, Diehl GW, Frackman A, Leffler J (2013) Medial prefrontal cortex lesions impair decision-making on a rodent gambling task: reversal by D1 receptor antagonist administration. Behav Brain Res 243:247–254. doi:10.1016/j.bbr.2013.01.018

Pascual R, Zamora-Leon SP (2007) Chronic (-)-deprenyl administration attenuates dendritic developmental impairment induced by early social isolation in the rat. Dev Neurosci 29(3):261–267. doi:10.1159/000096413

Paxinos G, Franklin KBG (2001) The mouse brain in stereotaxic coordinates, 2nd edn. Academic Press, San Diego

Paxinos G, Watson C (1998) The rat brain in stereotaxic coordinates, 4th edn. Academic Press, San Diego

Potegal M (2012) Temporal and frontal lobe initiation and regulation of the top-down escalation of anger and aggression. Behav Brain Res 231(2):386–395. doi:10.1016/j.bbr.2011.10.049

Potts GF, George MR, Martin LE, Barratt ES (2006) Reduced punishment sensitivity in neural systems of behavior monitoring in impulsive individuals. Neurosci Lett 397(1–2):130–134. doi:10.1016/j.neulet.2005.12.003

Raine A, Lencz T, Bihrle S, LaCasse L, Colletti P (2000) Reduced prefrontal gray matter volume and reduced autonomic activity in antisocial personality disorder. Arch Gen Psychiatry 57(2):119–127 **(discussion 128–119)**

Sagvolden T (2006) The alpha-2A adrenoceptor agonist guanfacine improves sustained attention and reduces overactivity and impulsiveness in an animal model of Attention-Deficit/Hyperactivity Disorder (ADHD). Behav Brain Funct BBF 2:41. doi:10.1186/1744-9081-2-41

Sanada LS, Sato KL, Machado NL, Carmo Ede C, Sluka KA, Fazan VP (2014) Cortex glial cells activation, associated with lowered mechanical thresholds and motor dysfunction, persists into adulthood after neonatal pain. Int J Dev Neurosci Off J Int Soc Dev Neurosci 35:55–63. doi:10.1016/j.ijdevneu.2014.03.008

Sandi C, Haller J (2015) Stress and the social brain: behavioural effects and neurobiological mechanisms. Nat Rev Neurosci 16(5):290–304. doi:10.1038/nrn3918

Schneider F, Habel U, Kessler C, Posse S, Grodd W, Muller-Gartner HW (2000) Functional imaging of conditioned aversive emotional responses in antisocial personality disorder. Neuropsychobiology 42(4):192–201

Schubert MI, Porkess MV, Dashdorj N, Fone KC, Auer DP (2009) Effects of social isolation rearing on the limbic brain: a combined behavioral and magnetic resonance imaging volumetry study in rats. Neuroscience 159(1):21–30. doi:10.1016/j.neuroscience.2008.12.019

Siegel A, Roeling TA, Gregg TR, Kruk MR (1999) Neuropharmacology of brain-stimulation-evoked aggression. Neurosci Biobehav Rev 23(3):359–389

Siever LJ (2008) Neurobiology of aggression and violence. The American journal of psychiatry 165(4):429–442. doi:10.1176/appi.ajp.2008.07111774

Skupio U, Tertil M, Sikora M, Golda S, Wawrzczak-Bargiela A, Przewlocki R (2015) Behavioral and molecular alterations in mice resulting from chronic treatment with dexamethasone: relevance to depression. Neuroscience 286:141–150. doi:10.1016/j.neuroscience.2014.11.035

Spitzer M, Fischbacher U, Herrnberger B, Gron G, Fehr E (2007) The neural signature of social norm compliance. Neuron 56(1):185–196. doi:10.1016/j.neuron.2007.09.011

Spivey JM, Shumake J, Colorado RA, Conejo-Jimenez N, Gonzalez-Pardo H, Gonzalez-Lima F (2009) Adolescent female rats are more resistant than males to the effects of early stress on prefrontal cortex and impulsive behavior. Dev Psychobiol 51(3):277–288. doi:10.1002/dev.20362

Takahashi A, Nagayasu K, Nishitani N, Kaneko S, Koide T (2014) Control of intermale aggression by medial prefrontal cortex activation in the mouse. PLoS One 9(4):e94657. doi:10.1371/journal.pone.0094657

Tebartz van Elst L, Hesslinger B, Thiel T, Geiger E, Haegele K, Lemieux L, Lieb K, Bohus M, Hennig J, Ebert D (2003) Frontolimbic brain abnormalities in patients with borderline personality disorder: a volumetric magnetic resonance imaging study. Biol Psychiatry 54(2):163–171

Tiihonen J, Rossi R, Laakso MP, Hodgins S, Testa C, Perez J, Repo-Tiihonen E, Vaurio O, Soininen H, Aronen HJ, Kononen M, Thompson PM, Frisoni GB (2008) Brain anatomy of persistent violent offenders: more rather than less. Psychiatry Res 163(3):201–212. doi:10.1016/j.pscychresns.2007.08.012

Toth M, Fuzesi T, Halasz J, Tulogdi A, Haller J (2010) Neural inputs of the hypothalamic "aggression area" in the rat. Behav Brain Res 215(1):7–20. doi:10.1016/j.bbr.2010.05.050

Toth M, Mikics E, Tulogdi A, Aliczki M, Haller J (2011) Post-weaning social isolation induces abnormal forms of aggression in conjunction with increased glucocorticoid and autonomic stress responses. Horm Behav 60(1):28–36. doi:10.1016/j.yhbeh.2011.02.003

Toth M, Tulogdi A, Biro L, Soros P, Mikics E, Haller J (2012) The neural background of hyper-emotional aggression induced by post-weaning social isolation. Behav Brain Res 233(1):120–129. doi:10.1016/j.bbr.2012.04.025

Tóth M, Halász J, Mikics E, Barsy B, Haller J (2008) Early social deprivation induces disturbed social communication and violent aggression in adulthood. Behav Neurosci 122(4):849–854. doi:10.1037/0735-7044.122.4.849

Tulogdi A, Toth M, Halasz J, Mikics E, Fuzesi T, Haller J (2010) Brain mechanisms involved in predatory aggression are activated in a laboratory model of violent intra-specific aggression. Eur J Neurosci 32(10):1744–1753. doi:10.1111/j.1460-9568.2010.07429.x

Tulogdi A, Biro L, Barsvari B, Stankovic M, Haller J, Toth M (2015) Neural mechanisms of predatory aggression in rats-implications for abnormal intraspecific aggression. Behav Brain Res 283:108–115. doi:10.1016/j.bbr.2015.01.030

Van De Werd HJ, Uylings HB (2008) The rat orbital and agranular insular prefrontal cortical areas: a cytoarchitectonic and chemoarchitectonic study. Brain Struct Funct 212(5):387–401. doi:10.1007/s00429-007-0164-y

van Praag H, Lucero MJ, Yeo GW, Stecker K, Heivand N, Zhao C, Yip E, Afanador M, Schroeter H, Hammerstone J, Gage FH (2007) Plant-derived flavanol (-)epicatechin enhances angiogenesis and retention of spatial memory in mice. J Neurosci Off J Soc Neurosci 27(22):5869–5878. doi:10.1523/jneurosci.0914-07.2007

Veit R, Lotze M, Sewing S, Missenhardt H, Gaber T, Birbaumer N (2010) Aberrant social and cerebral responding in a competitive reaction time paradigm in criminal psychopaths. Neuroimage 49(4):3365–3372. doi:10.1016/j.neuroimage.2009.11.040

Vollm B, Richardson P, McKie S, Reniers R, Elliott R, Anderson IM, Williams S, Dolan M, Deakin B (2010) Neuronal correlates and serotonergic modulation of behavioural inhibition and reward in healthy and antisocial individuals. J Psychiatr Res 44(3):123–131. doi:10.1016/j.jpsychires.2009.07.005

Wall VL, Fischer EK, Bland ST (2012) Isolation rearing attenuates social interaction-induced expression of immediate early gene protein products in the medial prefrontal cortex of male and female rats. Physiol Behav 107(3):440–450. doi:10.1016/j.physbeh.2012.09.002

Wang YC, Ho UC, Ko MC, Liao CC, Lee LJ (2012) Differential neuronal changes in medial prefrontal cortex, basolateral amygdala and nucleus accumbens after postweaning social isolation. Brain Struct Funct 217(2):337–351. doi:10.1007/s00429-011-0355-4

Wolansky T, Pagliardini S, Greer JJ, Dickson CT (2007) Immunohistochemical characterization of substance P receptor (NK(1)R)-expressing interneurons in the entorhinal cortex. J Comp Neurol 502(3):427–441

Wolf RC, Pujara MS, Motzkin JC, Newman JP, Kiehl KA, Decety J, Kosson DS, Koenigs M (2015) Interpersonal traits of psychopathy linked to reduced integrity of the uncinate fasciculus. Hum Brain Mapp 36(10):4202–4209. doi:10.1002/hbm.22911